# Epileptic Seizure Detection Based on Attitude Angle Signal of Wearable Device

Jiabing Wang, Dinghan Hu, *Member, IEEE*, Xiaoping Lai, Tao Jiang, Tiejia Jiang, Feng Gao, Pierre-Paul Vidal, and Jiuwen Cao, *Senior Member, IEEE*

***Abstract*— Wearable wristband device-based epilepsy detection has the merits of noninvasiveness, portability, low costs, and good environmental adaptability. However, attention has been paid to exploring the attitude angle signals collected by wearable devices for epilepsy detection. In this article, a systematic analysis of whether the wearable device-based attitude angle signals, particularly the PITCH and ROLL angles, can be applied to epilepsy seizure detection, is studied. The relationship among attitude angle signals, acceleration, and angular velocity signals at the feature level is analyzed, and the detection effectiveness of combining different attitude angle features for classifier training and testing is presented and discussed. The long-term recorded data were collected by wearable devices from 28 epileptic patients, of which 11 were from the Fourth Affiliated Hospital of Anhui Medical University and 17 from the Department of Neurology, Children's Hospital, Zhejiang University School of Medicine. Each recording includes the measurement of three-axis acceleration (ACC), three-axis gyroscope (GYR), ROLL, PITCH, surface electromyography (SEMG), and electrodermal activity (EDA), with at least one seizure recorded for each subject. Experimental results show that ROLL and PITCH angles can be utilized for epilepsy detection, with better performance than using ACC and GYR. Moreover, the attitude angle feature training by a long short-term memory (LSTM) network can achieve the highest accuracy and efficiency.**

Received 12 March 2024; revised 30 September 2024; accepted 24 October 2024. Date of current version 28 January 2025. This work was supported in part by the Natural Science Key Foundation of Zhejiang Province under Grant LZ24F030010 and Grant LQN25F030013, in part by the National Key Research and Development Program of China under Grant 2021YFE0100100 and Grant 2021YFE0205400, in part by the Zhejiang Provincial Natural Science Foundation under Grant LZ22F030002, and in part by the National Natural Science Foundation of China under Grant U1909209. The Associate Editor coordinating the review process was Dr. Yunjie Yang. *(Corresponding authors: Dinghan Hu; Jiuwen Cao.)*

This work involved human subjects or animals in its research. Approval of all ethical and experimental procedures and protocols was granted by the Children's Hospital, Zhejiang University School of Medicine under Application No. 2020-IRB-124, and the Fourth Affiliated Hospital of Anhui Medical University under Application No. PJ-YX2021-019.

Jiabing Wang, Dinghan Hu, Xiaoping Lai, and Jiuwen Cao are with Machine Learning and I-health International Cooperation Base of Zhejiang Province and the Artificial Intelligence Institute, Hangzhou Dianzi University, Hangzhou, Zhejiang 310018, China (e-mail: 1172598406@qq.com; hdh@hdu.edu.cn; laixp@hdu.edu.cn; jwcao@hdu.edu.cn).

Tao Jiang is with the Department of Neurosurgery and Anhui Public Health Clinical Center, First Affiliated Hospital of Anhui Medical University, Hefei, Anhui 230002, China (e-mail: jiangtao@ahmu.edu.cn).

Tiejia Jiang and Feng Gao are with the Department of Neurology, Children's Hospital, the National Clinical Research Center for Child Health, Zhejiang University School of Medicine, Hangzhou 310003, China (e-mail: jiangyouze@zju.edu.cn; epilepsy@zju.edu.cn).

Pierre-Paul Vidal is with the Plateforme d'Etude de la Sensorimotricité (PES), BioMedTech Facilities, Université Paris Cité, 75270 Paris, France (e-mail: pierre-paul.vidal@parisdescartes.fr).

Digital Object Identifier 10.1109/TIM.2025.3529058

***Index Terms*— Acceleration, angular velocity signal, attitude angle signal, long short-term memory (LSTM), multimodal signal analysis, seizure detection, wearable device.**

## I. Introduction

EPILEPSY is a serious neurological disorder that affects approximately 1% of the world's population [1], [2]. Due to the unpredictable and recurrent nature of epileptic seizures, the loss of muscle control and consciousness that accompany seizures can pose serious, even life-threatening risks of injury for patients. People with epilepsy are two to three times more likely to die than the general population [3], [4]. Video electroencephalography (EEG) in hospitalized patients is currently considered the gold standard for epilepsy analysis, but it is only available in hospitals or specialized epilepsy testing units, is not portable, and is costly and of limited duration [5], [6]. Wearable devices have better environmental adaptability and portability compared to video EEG, and comfort is ensured while the patient is wearing the device.

Wearable devices have better environmental adaptability and portability compared to video EEG, and comfort is ensured while the patient is wearing the device. The wearable device is widely used in various fields and plays an important role in epileptic seizure detection. During seizures, there tends to be more selectivity in the detection of seizure signals due to significant changes in the associated physiological signals. Various aspects of seizures can be assessed by non-EEG biosignals, including acceleration (ACC), electrodermal activity (EDA), body temperature, electromyography, or photoplethysmography (PPG) [7], [8], which have been used to detect epilepsy in either an unimodal or a multimodal form [9], [10], [11].

Among various non-EEG biosignals, ACC has been always used to detect epileptic seizures with motor symptoms, such as GTCS [12], [13]. An accelerometer is often considered the standard or minimum sensor configuration required to characterize human activity [14]. However, the acceleration signal is susceptible to external disturbances and can generate large noise spikes. The attitude angle signal, as a synthetic signal, is more stable compared to the acceleration signal, less sensitive to external disturbances, and has a faster response to changes in posture, but the contribution of the attitude angle signal to the detection of epileptic seizures has not been extensively investigated and analyzed.

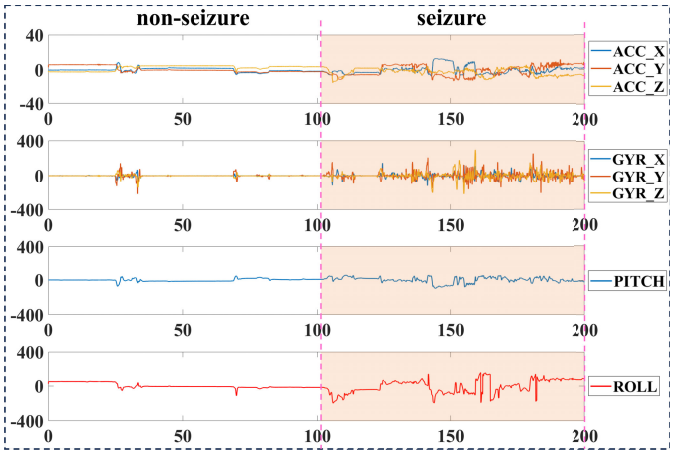


Fig. 1. Signals of three-axis ACC, three-axis GYR, and attitude angle (PITCH and ROLL).

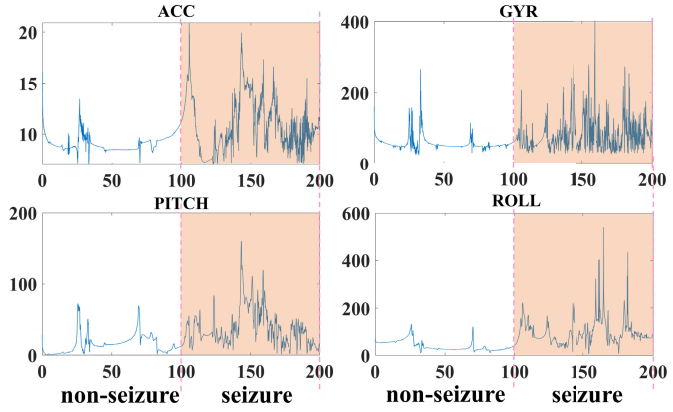


Fig. 2. Envelopes of synthetic acceleration, synthetic angular velocity, and attitude angle (PITCH and ROLL).

The attitude angle signal has been widely used in the fields of navigation, agriculture, and attitude detection [15], [16] and holds a significant research value and medical investigation significance in epileptic seizure detection. Attitude angle signals consist of the pitch angle signal (PITCH), yaw angle signal (YAW), and roll angle signal (ROLL), which describe the change in the rotation angle of the bracelet device around the $X$-, $Y$-, and $Z$-axes, respectively [17], [18]. This article mainly analyzed three-axis ACC, three-axis GYR, PITCH, and ROLL for seizure detection, as shown in Fig. 1. The attitude angle signal is derived from sensor fusion of a three-axis gyroscope and a three-axis accelerometer [19], defined as

$$\text{PITCH} = \tan^{-1}\left(\frac{-a_x}{\sqrt{a_y^2 + a_z^2}}\right) - g_y \times \triangle t. \tag{1}$$

$$\text{ROLL} = \tan^{-1}\left(\frac{-a_y}{a_x}\right) - g_x \times \triangle t \tag{2}$$

where $a_x$, $a_y$, and $a_z$ are the accelerations in the $X$-, $Y$-, and $Z$-axes, respectively; $g_x$, $g_y$, and $g_z$ are the angular velocities in the $X$-, $Y$-, and $Z$-axes, respectively; and $\triangle t$ is the sampling time interval.

The results of the envelope analysis of the four action classes of Fig. 1 are shown in Fig. 2. It can be seen that

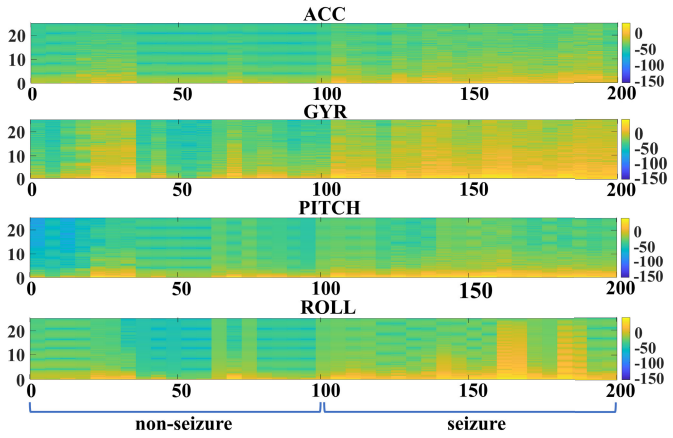


Fig. 3. Time–frequency plots of synthetic acceleration, synthetic angular velocity, and attitude angle (PITCH and ROLL).

all four action classes have more spikes present during the seizure, and the seizure event can be captured. However, for ACC and GYR, the number of spikes present in the nonseizure phase was significantly greater than for PITCH and ROLL, which is more resistant to interference in the nonseizure phase of epilepsy than in ACC and GYR. The results of the time–frequency plot analysis of Fig. 1 are shown in Fig. 3. It can be seen that the attitude angle signal has a significant rise in energy in the frequency range of 0–25 Hz during a seizure, and the amplitude of the rise in energy is significantly higher than ACC. When there is no seizure, the attitude angle signal does not show a wide range of energy enhancement compared to GYR because it has a better anti-interference ability. It can be seen that the attitude angle signal is less sensitive to external interference, has a faster response speed to attitude changes, and has a greater application prospect in seizure detection.

This article is the first to investigate the role of attitude angle signals for seizure detection, specifically focusing on the ROLL and PITCH. The six-modal signals (ACC, GYR, PITCH, ROLL, surface electromyography (SEMG), and EDA) are filtered in different ways to remove interfering components, and then relevant features are extracted and fused. Using unimodal and multimodal signals, three traditional classifiers are trained and compared, and the possibility of PITCH/ROLL replacing ACC/GYR for seizure detection is discussed. Besides, the proposed epilepsy detection algorithm based on multimodal signals and long short-term memory (LSTM) shows high detection accuracy and low complexity. The overall analysis flowchart is shown in Fig. 4.

## II. Methodology

### A. Data Acquisition

In this article, the data of 28 epileptic patients were researched, with 11 patients coming from the Fourth Affiliated Hospital of Anhui Medical University and 17 patients coming from the Department of Neurology, Children's Hospital, Zhejiang University School of Medicine. Informed consent was obtained from all participants and their legal guardians. Despite spending more time in a stationary state in the hospital environment compared to their daily lives, patients were not

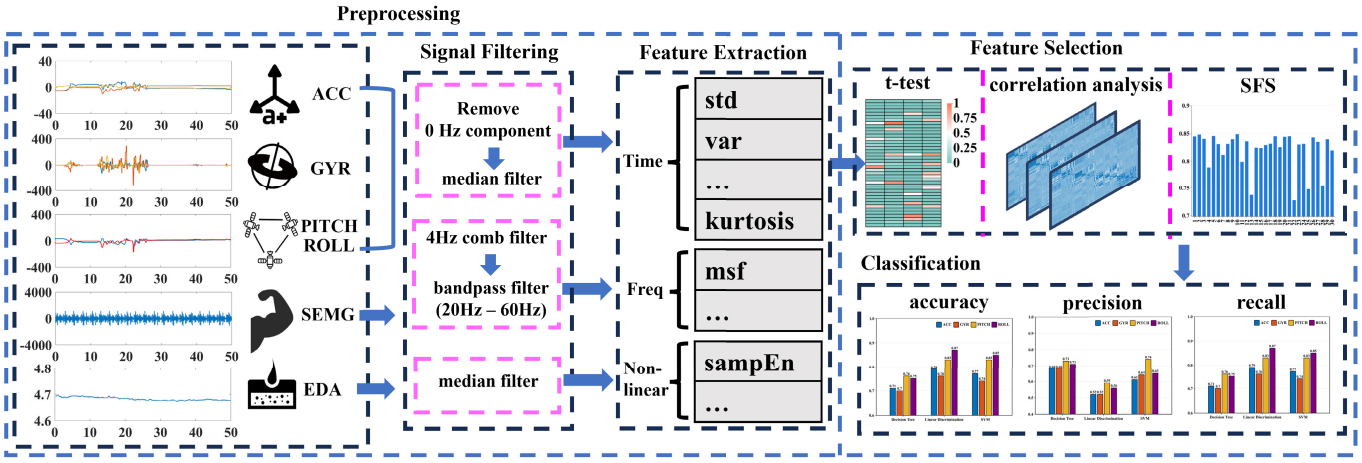


Fig. 4. Overall analysis flowchart.

completely immobile. All patients were recorded using identical wearable devices in both hospitals, and video EEG signals were simultaneously collected. Among 28 epileptic patients included in the analysis, 22 patients exhibited at least one seizure recorded, resulting in a cumulative total of 62 seizures. Each patient wears a wristband called "Biovital-P1," which consists of an "EMP sensor" and an "OPPO watch2." The application running in the OPPO watch can collect a variety of physiological signals from the wrist, including pulse, pulse rate variability, and blood sample signals from the OPPO watch, as well as nine modal physiological signals such as SEMG, EDA, ACC, and GYR from the EMP sensor, and the wristband also calculates the attitude angle signals from ACC and GYR. Raw data is stored as files in the local memory of the OPPO watch, while raw data can also be transferred in real time to the mobile phone for viewing and analysis when connected to Wi-Fi. The data stored in the wristband can be exported via USB or transferred to the cloud.

To compensate for time drift between the different devices, the clocks of both devices were synchronized before acquiring the physiological signals with the wristband corrected for time over a network. While acquiring the patient's physiological signals, both the wristband and EEG monitoring device recorded scalp EEG signals, which were then visually inspected by a clinical expert on EEG to mark seizure periods. The types of signals used in this article and the associated sampling frequencies are as follows: ACC at 50 Hz, GYR at 50 Hz, ROLL at 50 Hz, PITCH at 50 Hz, SEMG at 200 Hz, and EDA at 4 Hz. The details of the data are shown in Table I.

The ACC and GYR are obtained from the accelerometer and gyroscope inside the wristband, referring to the linear acceleration situation in three spatial dimensions and the angular velocity situation of the three spatial rotation axes of the wristband device, respectively. The PITCH and ROLL are signals obtained by sensor fusion with a three-axis gyroscope and a three-axis accelerometer. During seizures, patients are prone to some degree of limb jerking, and this motor phenomenon is readily reflected in features such as the time–frequency domain of action-like signals. SEMG refers to a signal that measures muscle activity. During a seizure, muscles usually contract and relax involuntarily, and this abnormal muscle activity produces noticeable changes in SEMG [20]. EDA refers to a signal that measures the surface electrical activity of the skin. During a seizure, skin conductance may change.

TABLE I

DETAILS OF DATA (F: FEMALE, M: MALE, Y: YEAR, M: MONTH, H: HOUR)

| Patient ID | Age | Gender | Num. of seizures | Record duration(H) |
|---|---|---|---|---|
| 1 | 10Y | M | 3 | 7.86 |
| 2 | 13Y | M | 1 | 9.53 |
| 3 | 6Y | F | 2 | 8 |
| 4 | 9Y2M | M | 1 | 4.65 |
| 5 | 7Y8M | F | 6 | 6.25 |
| 6 | 7Y3M | M | 5 | 7.26 |
| 7 | 1Y4M | F | 1 | 8.54 |
| 8 | 5Y11M | F | 1 | 8.7 |
| 9 | 2Y11M | F | 1 | 5.1 |
| 10 | 9Y | M | 5 | 7.8 |
| 11 | 7Y6M | F | 7 | 13.11 |
| 12 | 5M | F | 1 | 5.18 |
| 13 | 7Y | F | 5 | 8.3 |
| 14 | 11Y | M | 1 | 7.86 |
| 15 | 1Y2M | F | 1 | 5.16 |
| 16 | 12Y | M | 1 | 8 |
| 17 | 11Y | F | 9 | 6.4 |
| 18 | 2Y9M | F | 4 | 7.4 |
| 19 | 5Y2M | M | 1 | 0.96 |
| 20 | 7Y8M | M | 1 | 7.56 |
| 21 | 4Y9M | M | 3 | 3.66 |
| 22 | 5Y3M | M | 2 | 6.73 |
| 23 | 4Y11M | M | 0 | 3.68 |
| 24 | 9Y | M | 0 | 2.45 |
| 25 | 11Y | M | 0 | 3.05 |
| 26 | 6Y | M | 0 | 7.96 |
| 27 | 5Y | M | 0 | 9.45 |
| 28 | 5Y | M | 0 | 7.55 |
| Total | / | / | 62 | 188.15 |

## B. Signal Preprocessing

Since noise is mixed into the signal initially captured by the wristband, this article adopts different ways to remove noise for different types of signals, as follows.

1) *ACC, GYR, PITCH, and ROLL:* The noise is usually composed of regular human motion and artifacts. The 0-Hz component is first removed to calibrate the baseline, and then a median filter with a width of 10 Hz is used to remove artifacts.
2) *SEMG:* For SEMG signals, we first used a 4-Hz comb filter to remove noise from the device, and then a 20–60-Hz bandpass filter was adopted to remove low-frequency artifacts due to common movements.
3) *EDA:* Since galvanic skin activity is a slowly varying signal and may contain motion artifacts, a median filter was used to remove the interfering signal components from the galvanic skin.

### C. Feature Extraction and Selection

After data preprocessing, the data is sliced using a sliding window approach [5], [6], [21]. However, the study by Chung et al. [22] found that the size of the sliding window may directly or indirectly affect the final recognition accuracy. Considering the relevant factors such as time resolution and accuracy, we used a sliding window with a length of 4 s and an overlap rate of 50% and then calculated the features of each modal signal from the sliding window. In terms of feature selection, time-domain features are the best features for detecting epileptic seizures using accelerometers. It has low computational complexity and is suitable for real-time analysis. SEMG contains a higher frequency domain ratio during seizures compared to normal activity, and nonlinear features on EDA can characterize the changes in skin conductance levels. Therefore, time, frequency, and nonlinear domain features are extracted from each signal in this article.

Since ACC and GYR are three-channel signals, the synthesized acceleration signal ($a_{\text{norm}} = (a_x^2 + a_y^2 + a_z^2)^{1/2}$) and the synthesized angular velocity signal ($g_{\text{norm}} = (g_x^2 + g_y^2 + g_z^2)^{1/2}$) are first calculated from the three acceleration signals ($a_x$, $a_y$, $a_z$) and the three angular velocity signals ($g_x$, $g_y$, $g_z$) after the filtering operation. The relevant features for $a_{\text{norm}}$ and $g_{\text{norm}}$ are then computed using a sliding window approach. In addition to extracting the time, frequency, and nonlinear domain features, we also extracted the mean diagonal length feature, which was computed from the acceleration time series using recurrence plots by Böttcher et al. [5] and successfully applied to detect focal seizure motor epilepsy with tonic or clonic movements. For the attitude angle signals (PITCH and ROLL), since they belong to the action class of signals like ACC and GYR, we use the same types of features as for ACC and GYR (time domain, frequency domain, nonlinear domain, and mean diagonal length features). For SEMG, in addition to the time, frequency, and nonlinear domain features, the over-zero rate feature was also computed. Conradsen et al. [20] found that the over-zero rate feature was also useful in detecting epileptic seizures for SEMG signals. The final features used in this article are shown in the first column of Table II.

The use of multimodal signals will result in higher accuracy in detecting seizures compared to unimodal signals because multimodal signals provide more comprehensive information.

TABLE II
$p$-VALUES OF DIFFERENT FEATURES ON SIX-MODAL SIGNALS

| Features | ACC | GYR | PITCH | ROLL | SEMG | EDA |
|---|---|---|---|---|---|---|
| Maximum | **<0.05** | **<0.05** | 0.059 | **<0.05** | **<0.05** | **<0.05** |
| Minimum | **<0.05** | 0.928 | **<0.05** | **<0.05** | **<0.05** | **<0.05** |
| Peak | **<0.05** | **<0.05** | **<0.05** | **<0.05** | **<0.05** | **<0.05** |
| Peak-to-Peak | **<0.05** | **<0.05** | **<0.05** | **<0.05** | **<0.05** | **<0.05** |
| Mean | **<0.05** | **<0.05** | 0.871 | 0.813 | **<0.05** | **<0.05** |
| Average Amplitude | **<0.05** | **<0.05** | **<0.05** | **<0.05** | **<0.05** | **<0.05** |
| Root Amplitude | **<0.05** | **<0.05** | **<0.05** | **<0.05** | **<0.05** | **<0.05** |
| Variance | **<0.05** | **<0.05** | **<0.05** | **<0.05** | **<0.05** | 0.065 |
| Standard deviation | **<0.05** | **<0.05** | **<0.05** | **<0.05** | **<0.05** | **<0.05** |
| Root Mean Squart | **<0.05** | **<0.05** | **<0.05** | **<0.05** | **<0.05** | **<0.05** |
| Kurtosis | 0.145 | 0.195 | 0.069 | 0.767 | **<0.05** | **<0.05** |
| Skewness | **<0.05** | 0.515 | **<0.05** | **<0.05** | **<0.05** | 0.347 |
| Shape Factor | **<0.05** | **<0.05** | **<0.05** | **<0.05** | **<0.05** | **<0.05** |
| Peaking Factor | **<0.05** | **<0.05** | **<0.05** | **<0.05** | **<0.05** | **<0.05** |
| Pulse Factor | **<0.05** | **<0.05** | **<0.05** | **<0.05** | **<0.05** | **<0.05** |
| Margin Factor | **<0.05** | **<0.05** | **<0.05** | **<0.05** | **<0.05** | **<0.05** |
| Clearance Factor | **<0.05** | **<0.05** | **<0.05** | **<0.05** | **<0.05** | **<0.05** |
| Average frequency | **<0.05** | **<0.05** | **<0.05** | **<0.05** | **<0.05** | **<0.05** |
| Barycenter frequency | **<0.05** | **<0.05** | **<0.05** | **<0.05** | **<0.05** | **<0.05** |
| Rms frequency | **<0.05** | **<0.05** | **<0.05** | **<0.05** | 0.165 | **<0.05** |
| frequency standard deviation | **<0.05** | **<0.05** | **<0.05** | **<0.05** | **<0.05** | **<0.05** |
| Average power spectral density | **<0.05** | **<0.05** | **<0.05** | 0.332 | **<0.05** | **<0.05** |
| median frequency | **<0.05** | 0.119 | **<0.05** | **<0.05** | **<0.05** | **<0.05** |
| Sample Entropy | **<0.05** | **<0.05** | **<0.05** | **<0.05** | **<0.05** | **<0.05** |
| Fuzzy Entropy | **<0.05** | **<0.05** | **<0.05** | **<0.05** | 0.071 | **<0.05** |
| Approximate Entropy | 0.4347 | **<0.05** | **<0.05** | **<0.05** | **<0.05** | 0.091 |
| ZeroCrossing | / | / | / | / | **<0.05** | / |
| mean diagonal length | 0.136 | **<0.05** | 0.722 | 0.751 | / | / |

The fusion methods of multimode signals generally include early fusion and late fusion. The early fusion method is employed in this article, where relevant features are first extracted from each modal signal, and then all the features are combined to construct a new feature vector. The combined feature vector is subsequently used for training the relevant classifier [23].

To enhance the accuracy of subsequent model classification, it is necessary to conduct a feature screening operation to identify the most crucial features for constructing an appropriate feature set. The t-test was first used to analyze the degree of difference between the features of different signals during seizure and nonseizure epilepsy, with the significance levels expressed as $p$-values. Table II shows the $p$-values of different features on six-modal signals. $p < 0.05$ indicates that the feature is significant and retained in this article. These features are analyzed by correlation analysis to remove the redundant features with high correlation. The importance of features is subsequently ranked using the forward search method (SFS) to retain only the top-ranked important features, thereby reducing unnecessary features and mitigating overfitting caused by high dimensionality. This approach ensures efficient classification performance of the classifier. At least 20 features are retained for each modal signal in this article to train the classifier.

### D. LSTM Classifier

Recurrent neural networks (RNNs) are better at learning the fundamental representation of time-varying signals [24]. A multitude of extensions and variations of RNNs have been reported in the relevant academic literature, such as the Skip RNN [25], LSTM, gated recurrent units [26], and so on. A stochastic recurrent network that considers the long-term dependencies inherent in the data has been proposed by Goyal et al. [27]. Besides, LSTM networks have been

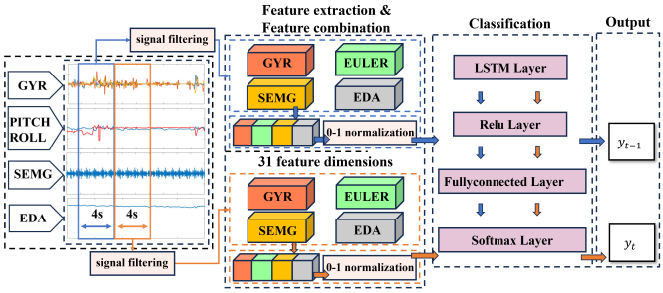


Fig. 5. LSTM-based seizure detection algorithm on the real-time monitoring component.

employed in various research, such as the modifier LSTM [28], external memory-based networks [29], and attention-based models [30]. After evaluating the benefits of each classification method, LSTM was adopted for seizure detection to further investigate the efficiency and feasibility of attitude angle signals in the real-time detection process, with the proposed LSTM-based seizure detection algorithm's workflow diagram shown in Fig. 5.

## III. Signal Analysis

### A. Analysis of Features

In this section, we focus on the analysis between the attitude angle, ACC, and GYR in terms of characterization to further explore the correlation among these signals. Here, we analyze the case of correlation between ACC, GYR, PITCH, and ROLL. The correlation heat maps on PITCH and ACC, PITCH and GYR, ROLL and ACC, and ROLL and GYR are drawn in Fig. 6. From the analysis of signal correlation among these four groups, it can be observed that the majority of time-domain features exhibit significant correlation, while a small portion of frequency-domain features also demonstrate noticeable correlation. Overall, there is a strong correlation between PITCH and ACC, as well as PITCH and GRY, with the same conclusion drawn for ROLL and ACC and ROLL and GRY. Fig. 7 shows the distribution of five representative features of the four action signals during the seizure and nonseizure phases. Since most of the features have a similar distribution, standard deviation and root mean square selected from the time-domain features, mean frequency and centroid frequency selected from the frequency-domain features, and fuzzy entropy features selected from the nonlinear features are chosen. The distribution of four types of action signals during different stages of epilepsy was elucidated through the examination of these five features. It is evident that the range of the feature distribution for the attitude angle signal is narrower compared to that of ACC and GYR. However, a more noticeable difference still exists between the features in the seizure and nonseizure phases. In terms of feature distribution across time, frequency, and nonlinear domains, the distribution of the attitude angle signal is very similar to that of ACC and GYR.

### B. Unimodal Signals-Based Machine Learning

To investigate whether attitude angle signals (PITCH and ROLL) have the same effect as ACC and GYR in detecting epileptic seizures, physiological signal data from a total of 18 epileptic patients with patient ID 1–18 were used. Conventional classifiers based on unimodal signals, including Tree, SVM, and linear discriminant (LDA), were constructed and compared. Experiments were conducted on patient IDs 1–18, with a total of 3197 samples. The dataset was divided into a training set (2558 samples) and a testing set (639 samples) with a ratio of 8:2. And tenfold cross-validation was applied to the training set for the most optimal model selection, resulting in 256 samples for validation in each round. Three main indicators of accuracy, precision, and recall were used to judge the performance of the model. The comparisons of performance results of the three different classifiers are shown in Table III. The PITCH-based trained LDA classifier achieved 78.20% accuracy, 83.20% precision, and 58.70% recall. Compared to ACC and GYR, it is 3.8% and 4.6% higher in accuracy, 4.7% and 7% higher in precision, and 7.1% and 7% higher in recall. The LDA classifier trained on ROLL achieved 78.70% accuracy, 87.10% precision, and 56.40% recall. Compared to ACC and GYR, it is 4.3% and 5.1% higher in accuracy, 8.6% and 10.9% higher in precision, and 4.8% and 4.7% higher in recall.

TABLE III
Comparison Results of Traditional Classifiers Based on Unimodal Signals

| Training results | ACC | GYR | PITCH | ROLL |
|---|---|---|---|---|
| (Tree) Accuracy | 75.30% | 74.90% | 79.30% | 78.60% |
| (Tree) Precision | 70.60% | 69.90% | 75.50% | 75.30% |
| (Tree) Recall | 68.40% | 68.20% | 73.00% | 71.30% |
| (SVM) Accuracy | 76.50% | 76.00% | 82.80% | 80.80% |
| (SVM) Precision | 76.70% | 74.00% | 82.50% | 84.80% |
| (SVM) Recall | 61.20% | 64.10% | 73.80% | 64.50% |
| (LDA) Accuracy | 74.40% | 73.60% | 78.20% | 78.70% |
| (LDA) Precision | 78.50% | 76.20% | 83.20% | 87.10% |
| (LDA) Recall | 51.60% | 51.70% | 58.70% | 56.40% |

It can be seen that PITCH and ROLL outperform ACC and GYR in terms of accuracy, precision, and recall of Tree, SVM, and LDA, which is also because the attitude angle signal is a signal obtained by fusing the sensors of a three-axis gyroscope and a three-axis accelerometer. Therefore, it has the same characteristics as ACC and GYR. The above results demonstrate that the attitude angle signals (PITCH and ROLL) can be used for seizure detection and are superior to ACC or GYR in the unimodal signals-based traditional classification model.

### C. Multimodal Signals-Based Machine Learning

In Section III-C, we found that PITCH and ROLL significantly outperform ACC and GYR when the unimodal signal is used to train the classifier. Given that the majority of epilepsy detection systems currently in use leverage multimodal signals for seizure detection, our study aims to examine the effects of incorporating PITCH and ROLL data into the combination of ACC and GYR multimodal signals on the overall performance of classifiers.

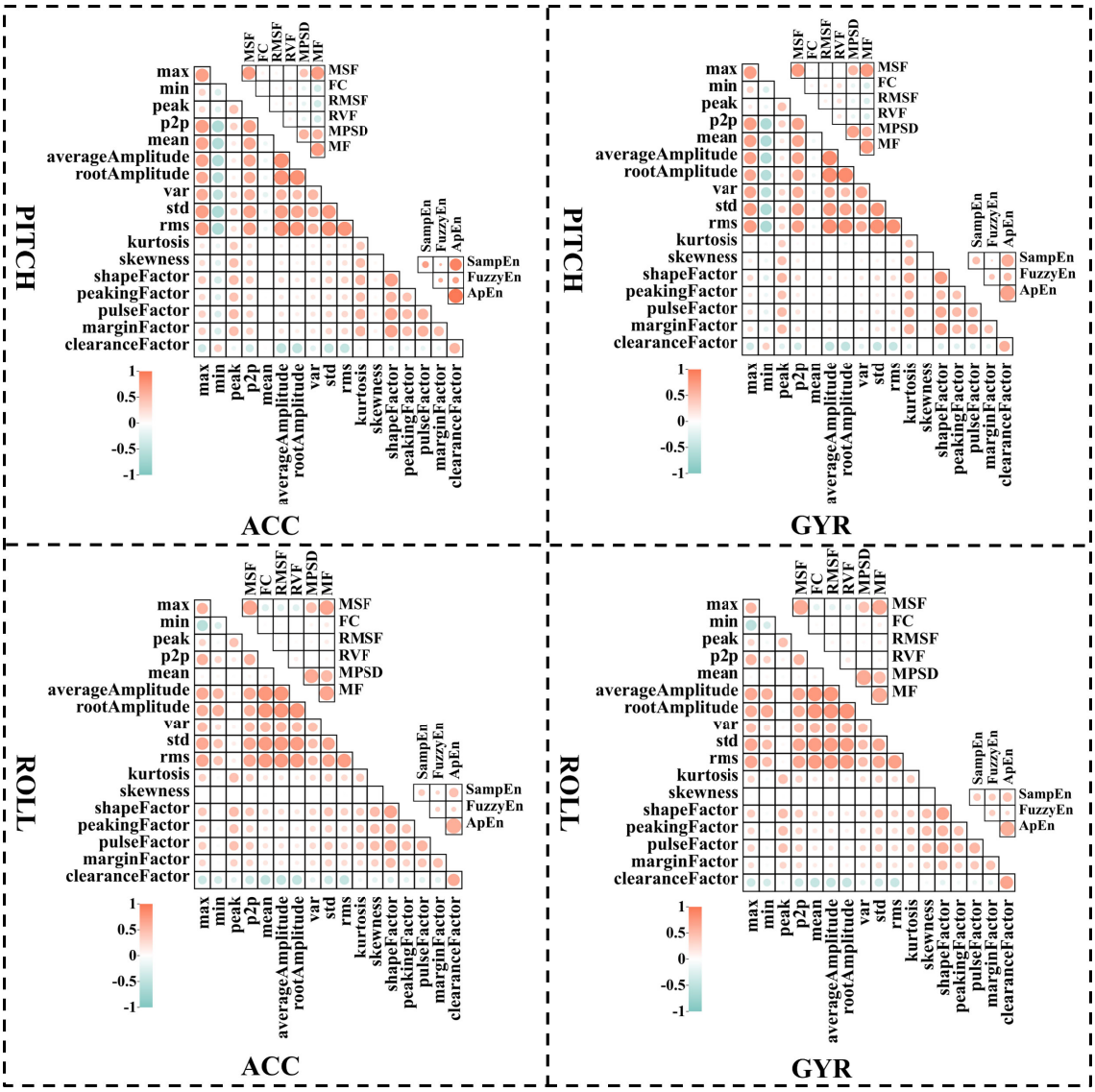


Fig. 6. Correlation heat map on PITCH and ACC, PITCH and GYR, ROLL and ACC, and ROLL and GYR.

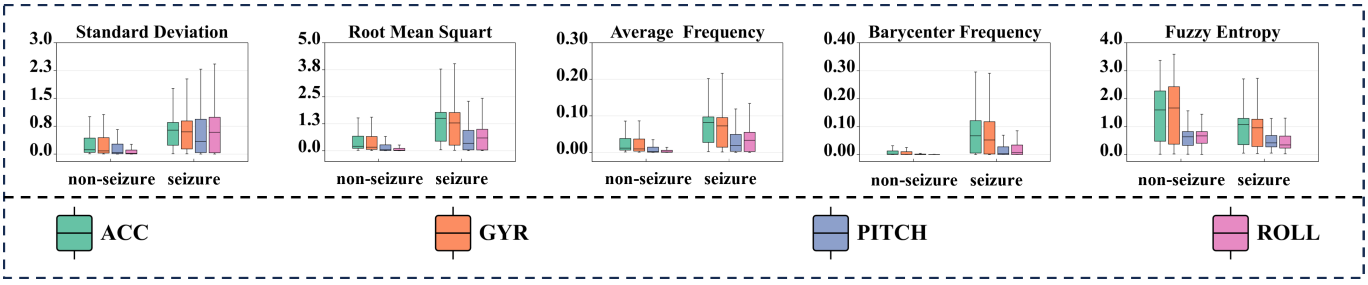


Fig. 7. Box plot of feature distribution on ACC, GYR, PITCH, and ROLL.

We define the signal types used in Combination 1 as ACC + GYR + SEMG + EDA, the signal types used in Combination 2 as ACC + GYR + PITCH + SEMG + EDA, the signal types used in Combination 3 as ACC + GYR + ROLL + SEMG + EDA, and the signal types used in Combination 4 as ACC + GYR + PITCH + ROLL + SEMG + EDA. The comparison results of traditional classifiers based on multimodal signals are shown in Table IV. It is clear that for all three classifiers (Tree, SVM, and LDA), when the PITCH is added alone (Combination 2) or the ROLL is added alone (Combination 3), the classifiers outperform Combination 1 on accuracy, precision, and recall. When both PITCH and ROLL are added to Combination 1 (Combination 4), some of the classifiers do not perform as well as Combination 2 or Combination 3, but the overall performance is still better than Combination 1 (without the PITCH or ROLL).

TABLE IV
COMPARISON RESULTS OF TRADITIONAL CLASSIFIERS BASED ON MULTIMODAL SIGNALS

| Training results | ACC+GYR+ SEMG+EDA | ACC+GYR+ PITCH+ SEMG+EDA | ACC+GYR+ ROLL+ SEMG+EDA | ACC+GYR+ PITCH+ROLL+ SEMG+EDA |
|---|---|---|---|---|
| (Tree) Accuracy | 89.40% | 90.60% | 91% | 90.70% |
| (Tree) Precision | 87.10% | 88.60% | 89.90% | 88.60% |
| (Tree) Recall | 86.90% | 88.60% | 90.60% | 88.90% |
| (SVM) Accuracy | 93.40% | 95.50% | 95% | 95.10% |
| (SVM) Precision | 92.90% | 95.80% | 95.30% | 95.30% |
| (SVM) Recall | 90.90% | 93.30% | 92.20% | 92.70% |
| (LDA) Accuracy | 87.10% | 88.50% | 89.60% | 88.80% |
| (LDA) Precision | 90.30% | 92.50% | 95.10% | 90.70% |
| (LDA) Recall | 76.70% | 78.20% | 78.70% | 81.10% |

Taking the SVM classifier as an example, the SVM classifier trained based on Combination 2 achieved 95.5% accuracy, 95.8% precision, and 95.3% recall, which is 2.1% higher in accuracy, 2.9% higher in precision, and 2.4% higher in recall than the SVM classifier trained based on Combination 1. The SVM classifier trained based on Combination 3 achieved 95% accuracy, 95.3% precision, and 92.2% recall, which provides 1.6% higher accuracy, 2.4% higher precision, and 1.3% higher recall than the SVM classifier trained based on Combination 1. The SVM classifier trained based on Combination 4 achieved 95.1% accuracy, 95.3% precision, and 92.7% recall, which is 1.7% higher in accuracy, 2.4% higher in precision, and 1.8% higher in recall than the SVM classifier trained based on Combination 1. Similar results were seen for Tree and LDA, where the classifiers trained with Combination 2, Combination 3, and Combination 4 outperformed the classifier trained with Combination 1 in all three metrics. It can be concluded that the introduction of the PITCH and ROLL has a certain improvement on the classification effect of the classifier.

### *D. Analysis of the Possibility of Attitude Angle Signals Replacing ACC and GYR*

By observing and analyzing the results of the performance of different modal signal combinations in the three classifiers, experimental results in the previous section prove that the PITCH and ROLL outperform the ACC and GYR in seizure detection. This section provides an in-depth analysis of the PITCH and ROLL and investigates the possibility of replacing the ACC and GYR with the PITCH and ROLL.

To research whether the attitude angle signal can replace ACC and GYR for seizure detection analysis in epilepsy, here the modal signal types used in Combination 1 are defined as ACC, GYR, SEMG, and EDA; the signal types used in Combination 2 are PITCH, GYR, SEMG, and EDA (PITCH replaces ACC); the signal types used in Combination 3 are ACC, PITCH, SEMG, and EDA (PITCH replaces GYR); Combination 4 uses PITCH, SEMG, and EDA (PITCH replaces ACC and GYR); Combination 5 uses ROLL, GYR, SEMG, and EDA (ROLL replaces ACC); Combination 6 uses ACC, ROLL, SEMG, and EDA (ROLL replaces GYR); Combination 7 uses ROLL, SEMG, and EDA (ROLL replaces ACC and GYR).

TABLE V
COMPARISON RESULTS OF TRADITIONAL CLASSIFIERS WITH THE PITCH REPLACING ACC/GYR

| Training results | ACC+GYR+ SEMG+EDA | PITCH+GYR+ SEMG+EDA | ACC+PITCH+ SEMG+EDA | PITCH+ SEMG+EDA |
|---|---|---|---|---|
| (Tree) Accuracy | 89.40% | 91.60% | 90.70% | 89.90% |
| (Tree) Precision | 87.10% | 90.00% | 89.20% | 88.00% |
| (Tree) Recall | 86.90% | 89.30% | 88.10% | 87.30% |
| (SVM) Accuracy | 93.40% | 95.70% | 95.20% | 94.90% |
| (SVM) Precision | 92.90% | 95.70% | 95.50% | 94.70% |
| (SVM) Recall | 90.90% | 93.80% | 92.70% | 92.70% |
| (LDA) Accuracy | 87.10% | 89.00% | 88.60% | 85.70% |
| (LDA) Precision | 90.30% | 91.70% | 92.30% | 87.80% |
| (LDA) Recall | 76.70% | 80.60% | 78.70% | 75.60% |

TABLE VI
COMPARISON RESULTS OF TRADITIONAL CLASSIFIERS WITH THE ROLL REPLACING ACC/GYR

| Training results | ACC+GYR+ SEMG+EDA | ROLL+GYR+ SEMG+EDA | ACC+ROLL+ SEMG+EDA | ROLL+ SEMG+EDA |
|---|---|---|---|---|
| (Tree) Accuracy | 89.40% | 91.30% | 90.50% | 89.40% |
| (Tree) Precision | 87.10% | 89.10% | 88.70% | 87.50% |
| (Tree) Recall | 86.90% | 89.70% | 88.20% | 86.60% |
| (SVM) Accuracy | 93.40% | 95.20% | 95.00% | 93.80% |
| (SVM) Precision | 92.90% | 95.70% | 95.00% | 93.50% |
| (SVM) Recall | 90.90% | 92.50% | 92.70% | 91.20% |
| (LDA) Accuracy | 87.10% | 89.50% | 88.70% | 87.40% |
| (LDA) Precision | 90.30% | 93.00% | 92.60% | 92.30% |
| (LDA) Recall | 76.70% | 80.40% | 78.60% | 75.60% |

The results of each signal combination approach trained in tree classification, SVM, and linear discrimination are shown in Tables V and VI.

From the results, we can see that in Combination 2 (PITCH instead of ACC), Combination 3 (PITCH instead of GYR), Combination 5 (ROLL instead of ACC), and Combination 6 (ROLL instead of GYR), the three metrics of accuracy, precision, and recall are significantly higher than the results in Combination 1, and there is a significant improvement in the classification efficiency of the classifiers. Combination 4 (PITCH replaces ACC and GYR) does not show a significant improvement in tree classification compared to Combination 1, and SVM shows an improvement of about 1%–2%, but there is a more significant decrease in linear discrimination instead. Combination 7 (ROLL replaces ACC and GYR) does not show a large gap in the metrics of the three classifiers compared to Combination 1.

In the study by Conradsen et al., the features extracted from the ACC, GYR, and SEMG were used to train the SVM classifier model, and the final classifier was 91% accurate [31]. In the study by Zsom et al. [32], features extracted from ACC, EDA, body temperature, and heart rate signals were used to train the XGBoost model, and the model achieved a classification performance of 78% accuracy. In the study by Vieluf et al. [33], features extracted from EDA, body temperature, and heart rate signals were used to train a machine learning model, and the cross-validated machine learning model had an accuracy of 0.69, a sensitivity of 0.68, and

a specificity of 0.75. In a study by Heldberg et al. [12], using ACC and EDA to detect epileptic seizures with motor symptoms, the final KNN classifier had a sensitivity of 89.1% and a specificity of 93.1%. It can be seen that the attitude angle signal instead of the ACC and GYR signal combination approach leads to better training results as well as higher training metrics for the classifier.

### *E. LSTM-Based Seizure Detection*

In this section, a wearable device-based algorithm for detecting epileptic seizures using LSTM is proposed. The proposed model consists of four layers: signal input layer, feature extraction layer, early fusion layer, and classifier layer.

In the feature extraction layer, traditional features of the signal including time-domain features, frequency-domain features, and nonlinear domain features are extracted. In the early fusion layer, the features of each modality are combined into a feature vector. Since the training and testing set features are normalized using the 0–1 normalization method, and the normalization parameters are stored before the LSTM classifier is trained. Hence, the feature vectors must be normalized using the previously stored normalization parameters from the training step after the feature vectors are collated in the early fusion layer. In the classifier layer, LSTM was adopted, consisting of one LSTM layer (40 hidden units), one Relu activation layer, one fully connected layer, and one softmax layer. During the training process, the dataset is randomly divided into a training set and a testing set, where the testing set is 20% of the total data, and tenfold cross-validation is used to train the classifier to prevent overfitting of the classifier. The ADAM optimizer with binary cross-entropy loss function is used to ensure the classification efficiency of the classifier as much as possible [34]. To further demonstrate the effectiveness of the proposed method, we collected 500 samples from each of patient IDs 19–28, resulting in an additional testing set comprising 5000 samples (including both seizure and nonseizure). The performance is measured by the mean square error, which is given by the following equation:

$$\mathrm{MSE} = \frac{1}{n}\sum_{i=1}^{n}(x_i - y_i)^2$$

where $n$ is the number of samples in the testing set, $x_i$ is the true label of the sample, and $y_i$ is the label predicted by the classifier. To optimize the performance of the classifier and to prevent the classifier from overfitting, the internal hyperparameters of the LSTM classifier are adjusted by grid search. The smaller the MSE, the better the model performance. When the number of LSTM layers is 1 with 40 hidden units and the learning rate is set to 0.01, the MSE is 0.08674, which achieves the best performance.

Three LSTM classifiers using different signal combinations are trained, with the specification as follows: classifier 1 for the signal types ACC, GYR, SEMG, and EDA; classifier 2 for the signal types PITCH, GYR, SEMG, and EDA; and classifier 3 for the signal types ROLL, GYR, SEMG, and EDA. The model evaluation metrics are the number of seizures detected, false alarm rate, and accuracy. The data used for model training comes from patient IDs 1–18 (3197 samples), in which 2558 samples were for tenfold cross-validation, and the long-term data from patient IDs 19–28 were reserved for testing. Table VII shows the test results by these three LSTM classifiers on the data with seven labeled seizure events. For classifier 1, four seizures were successfully detected with an overall classification accuracy of 80.1%, and a total of 11 false alarms occurred in the offline data with a cumulative length of 30.24 h, with the false alarm rate of 8.73/24 h. For classifier 2, five seizures were successfully detected with a classification accuracy of 83.4%, and a total of 10 false alarms occurred in the offline data with a cumulative length of 28.36 h, with the false alarm rate of 8.46/24 h. For classifier 3, seizures were successfully detected four times with an accuracy of 82.5%, and a total of 9 false alarms occurred in the offline signals with a cumulative length of 25.36 h, with the false alarm rate of 8.51/24 h.

TABLE VII
TEST RESULTS ON DIFFERENT MULTIMODAL SIGNAL COMBINATION

| Detection Methods | ACC+GYR+ SEMG+EDA | PITCH+GYR+ SEMG+EDA | ROLL+GYR+ SEMG+EDA |
|---|---|---|---|
| Number of Epilepsy Tests | 4 | 5 | 4 |
| Accuracy | 80.1% | 83.4% | 82.5% |
| False Alarm Rate | 8.73/24h | 8.46/24h | 8.51/24h |
| Detection Methods | Paul Boon et al [35] | Judith van Andel et al [36] | Yangbin Ge et al [37] |
| Accuracy | 81.8% | 79.0% | 82.6% |
| False Alarm Rate | 11.76/24h | 12/24h | 8.63/24h |

In a study by Boon et al. [35], an ECG-based action-based seizure detection system was developed with a final accuracy of 81.8% and a false alarm rate of 11.76/24 h. The study by van Andel et al. [36] used acceleration signals and electromyographic signals for action-based seizure detection with a final median accuracy of 79% and a median false alarm rate of 12/24 h. In a study by Ge et al. [37], the ACC signal, angular velocity signal (GYR), SEMG signal, and EDA signal were used to detect epileptic seizures, and the sensitivity of the final classifier was 82.6%, with a false alarm rate of 8.63/24 h. The comparison with the results of others shows that the proposed LSTM-based seizure detection algorithm, using attitude angle signals instead of ACC and GYR signals, has a final false alarm rate index in a reasonable range and achieves better accuracy.

The detection efficiency results shown in Table VII indicate that when PITCH and ROLL replace ACC, the accuracy is improved to some extent and the false alarm rate does not change much, which shows that PITCH and ROLL can indeed be used for seizure detection and that PITCH and ROLL can be used in place of ACC. Since there are not many studies using GYR, a real-time monitoring model that replaces GYR with attitude angle signaling was not developed here. However, due to the high correlation among the four signals ACC, GYR, PITCH, and ROLL in terms of features, as illustrated in

TABLE VIII
TEST RESULTS FOR PATIENT IDS 19–28

| Patient ID | Accuracy |
|---|---|
| 19 | 89.2% |
| 20 | 80.8% |
| 21 | 77.6% |
| 22 | 82.2% |
| 23 | 84.8% |
| 24 | 93.2% |
| 25 | 90.6% |
| 26 | 97.8% |
| 27 | 97.6% |
| 28 | 76.4% |

the previous sections, we have demonstrated that the attitude angle signal has the potential to replace GYR based on three metrics from three classifiers. Combining these results with the findings presented in this section, we can conclude that both PITCH and ROLL can also serve as substitutes for GYR in seizure detection for epilepsy. In the long term, attitude angle signals have a greater potential for epileptic seizure detection, and attitude angle signals characterized by both ACC and GYR signals remain open for more in-depth study in the future.

In the epileptic seizure detection system, employing traditional features in time, frequency, and nonlinear domains for classifier training with a sliding window overlap rate of 0% leads to a significant increase in false alarm rates during actual performance. However, this issue can be mitigated by incorporating deep learning techniques and increasing the overlap rate.

Patient-specific testing experiments are conducted on each of patient IDs 19–28, where the number of LSTM layers is 1 with 40 hidden units and the learning rate is set to 0.01. For each patient, 500 samples are used to test, with the results shown in Table VIII. The proposed method achieves the best performance with 97.8% accuracy for patient ID 26. Among patient IDs 19–28, four patients achieved the test accuracy exceeding 90%. These results demonstrate the superior classification performance and generalization ability of the proposed method.

## IV. CONCLUSION

This article explores the usability of attitude angle signals (PITCH and ACC) for epileptic seizure monitoring and conducts an in-depth analysis of the feature level of the signals. Through three classifiers (Tree, SVM, and LDA), it is proved that the attitude angle signal can be used for seizure detection and outperforms the commonly used ACC signal as well as the GYR signal in terms of the indicators of accuracy, precision, and recall. Besides, the proposed LSTM-based seizure monitoring algorithm using multimodal signals collected from wearable devices and a multigroup comparison experiment also demonstrates the usability of attitude angle signals. In the LSTM-based seizure detection system, three different signal combination methods are selected and three different LSTM classifiers are trained. It is concluded that the attitude angle signals (PITCH and ROLL) replace the ACC to realize the seizure detection of epilepsy by the two metrics of accuracy and false alarm rate.

Since the attitude angle signal is a single-channel signal, while ACC and GYR are three-channel signals, the algorithmic processing of the attitude angle signal in the preprocessing step is more efficient in terms of preprocessing speed. Consequently, there remains untapped potential for further exploration of attitude angle signals in seizure detection for epilepsy. This article demonstrates the viability of utilizing attitude angle signaling for seizure detection and offers additional options for future research in epilepsy by expanding the range of available detection signals.

## ACKNOWLEDGMENT

All the patients provided informed consent before inclusion in the study.

## REFERENCES

[1] M. Miloševic et al., "Automated detection of tonic–clonic seizures using 3-D accelerometry and surface electromyography in pediatric patients," *IEEE J. Biomed. Health Informat.*, vol. 20, no. 5, pp. 1333–1341, Sep. 2016.

[2] L. Dong, G. Li, C. Tian, L. Lin, Y. Gao, and Y. Zheng, "Design of submillimeter magnetic stimulation instrumentation and its targeted inhibitory effect on rat model of epilepsy," *IEEE Trans. Instrum. Meas.*, vol. 70, pp. 1–8, 2021.

[3] A. A. Kabanov and A. I. Shchelkanov, "Development of a wearable inertial system for motor epileptic seizure detection," in *Proc. 14th Int. Sci.-Tech. Conf. Actual Problems Electron. Instrum. Eng. (APEIE)*, Novosibirsk, Russia, Oct. 2018, pp. 339–342.

[4] M. N. A. Tawhid, S. Siuly, and T. Li, "A convolutional long short-term memory-based neural network for epilepsy detection from EEG," *IEEE Trans. Instrum. Meas.*, vol. 71, pp. 1–11, 2022.

[5] S. Böttcher et al., "Intra- and inter-subject perspectives on the detection of focal onset motor seizures in epilepsy patients," *Sensors*, vol. 22, no. 9, p. 3318, Apr. 2022.

[6] M. Nasseri et al., "Ambulatory seizure forecasting with a wrist-worn device using long-short term memory deep learning," *Sci. Rep.*, vol. 11, no. 1, p. 21935, Nov. 2021.

[7] M. Glasstetter et al., "Identification of ictal tachycardia in focal motor- and non-motor seizures by means of a wearable PPG sensor," *Sensors*, vol. 21, no. 18, p. 6017, Sep. 2021.

[8] M.-Z. Poh, T. Loddenkemper, N. C. Swenson, S. Goyal, J. R. Madsen, and R. W. Picard, "Continuous monitoring of electrodermal activity during epileptic seizures using a wearable sensor," in *Proc. Annu. Int. Conf. IEEE Eng. Med. Biol.*, Aug. 2010, pp. 4415–4418.

[9] A. Ulate-Campos, F. Coughlin, M. Gaínza-Lein, I. S. Fernández, P. L. Pearl, and T. Loddenkemper, "Automated seizure detection systems and their effectiveness for each type of seizure," *Seizure*, vol. 40, pp. 88–101, Aug. 2016.

[10] A. Van De Vel et al., "Non-EEG seizure detection systems and potential SUDEP prevention: State of the art," *Seizure*, vol. 41, pp. 141–153, Oct. 2016.

[11] F. Chen, I. Chen, M. Zafar, S. R. Sinha, and X. Hu, "Seizures detection using multimodal signals: A scoping review," *Physiological Meas.*, vol. 43, no. 7, Jul. 2022, Art. no. 07TR01.

[12] B. E. Heldberg, T. Kautz, H. Leutheuser, R. Hopfengärtner, B. S. Kasper, and B. M. Eskofier, "Using wearable sensors for semiology-independent seizure detection–towards ambulatory monitoring of epilepsy," in *Proc. 37th Annu. Int. Conf. IEEE Eng. Med. Biol. Soc. (EMBC)*, Aug. 2015, pp. 5593–5596.

[13] C. Dong et al., "A two-layer ensemble method for detecting epileptic seizures using a self-annotation bracelet with motor sensors," *IEEE Trans. Instrum. Meas.*, vol. 71, pp. 1–13, 2022.

[14] C. Ma et al., "Quantitative assessment of essential tremor based on machine learning methods using wearable device," *Biomed. Signal Process. Control*, vol. 71, Jan. 2022, Art. no. 103244.

[15] Y. Dong, Y. Zhang, and J. Ai, "Full-altitude attitude angles envelope and model predictive control-based attitude angles protection for civil aircraft," *Aerosp. Sci. Technol.*, vol. 55, pp. 292–306, Aug. 2016.

[16] H. Tian, Y. Liu, J. Zhou, Y. Wang, J. Wang, and W. Zhang, "Attitude angle compensation for a synchronous acquisition method based on an MEMS sensor," *Sensors*, vol. 19, no. 3, p. 483, Jan. 2019.

[17] J. L. Ackerman, W. R. Proffit, D. M. Sarver, M. B. Ackerman, and M. R. Kean, "Pitch, roll, and yaw: Describing the spatial orientation of dentofacial traits," *Amer. J. Orthodontics Dentofacial Orthopedics*, vol. 131, no. 3, pp. 305–310, Mar. 2007.

[18] K. D. Kumar and K. Kumar, "Satellite pitch and roll attitude maneuvers through very short tethers," *Acta Astronautica*, vol. 44, nos. 5–6, pp. 257–265, Mar. 1999.

[19] Y. Liu, N. Noguchi, and K. Ishii, "Development of a low-cost IMU by using sensor fusion for attitude angle estimation," *IFAC Proc. Volumes*, vol. 47, no. 3, pp. 4435–4440, 2014.

[20] I. Conradsen, S. Beniczky, K. Hoppe, P. Wolf, and H. B. D. Sorensen, "Automated algorithm for generalized tonic–clonic epileptic seizure onset detection based on sEMG zero-crossing rate," *IEEE Trans. Biomed. Eng.*, vol. 59, no. 2, pp. 579–585, Feb. 2012.

[21] N. Pradhan, S. Rajan, A. Adler, and C. Redpath, "Classification of the quality of wristband-based photoplethysmography signals," in *Proc. IEEE Int. Symp. Med. Meas. Appl. (MeMeA)*, May 2017, pp. 269–274.

[22] S. Chung, J. Lim, K. J. Noh, G. Kim, and H. Jeong, "Sensor data acquisition and multimodal sensor fusion for human activity recognition using deep learning," *Sensors*, vol. 19, no. 7, p. 1716, Apr. 2019.

[23] B. Nakisa, M. N. Rastgoo, A. Rakotonirainy, F. Maire, and V. Chandran, "Automatic emotion recognition using temporal multimodal deep learning," *IEEE Access*, vol. 8, pp. 225463–225474, 2020.

[24] D. Jyotishi and S. Dandapat, "An LSTM-based model for person identification using ECG signal," *IEEE Sensors Lett.*, vol. 4, no. 8, pp. 1–4, Aug. 2020.

[25] V. Campos, B. Jou, X. Giro-I-Nieto, J. Torres, and S.-F. Chang, "Skip RNN: Learning to skip state updates in recurrent neural networks," 2017, *arXiv:1708.06834*.

[26] K. Greff, R. K. Srivastava, J. Koutník, B. R. Steunebrink, and J. Schmidhuber, "LSTM: A search space Odyssey," *IEEE Trans. Neural Netw. Learn. Syst.*, vol. 28, no. 10, pp. 2222–2232, Oct. 2016.

[27] A. Goyal, A. Sordoni, M.-A. Côté, N. R. Ke, and Y. Bengio, "Z-forcing: Training stochastic recurrent networks," in *Proc. Adv. Neural Inf. Process. Syst.*, vol. 30, Nov. 2017, pp. 6713–6723.

[28] G. Melis, T. Kočiskỳ, and P. Blunsom, "Mogrifier LSTM," 2019, *arXiv:1909.01792*.

[29] S. Sukhbaatar, A. Szlam, J. Weston, and R. Fergus, "End-to-end memory networks," in *Proc. Adv. Neural Inf. Process. Syst.*, vol. 28, Dec. 2015, pp. 2440–2448.

[30] D. Bahdanau, K. Cho, and Y. Bengio, "Neural machine translation by jointly learning to align and translate," 2014, *arXiv:1409.0473*.

[31] I. Conradsen, S. Beniczky, P. Wolf, J. Henriksen, T. Sams, and H. B. D. Sorensen, "Seizure onset detection based on a uni- or multi-modal intelligent seizure acquisition (UISA/MISA) system," in *Proc. Annu. Int. Conf. IEEE Eng. Med. Biol.*, Aug. 2010, pp. 3269–3272.

[32] A. Zsom et al., "Ictal autonomic activity recorded via wearable-sensors plus machine learning can discriminate epileptic and psychogenic nonepileptic seizures," in *Proc. 41st Annu. Int. Conf. IEEE Eng. Med. Biol. Soc. (EMBC)*, Jul. 2019, pp. 3502–3506.

[33] S. Vieluf et al., "Seizure-related differences in biosignal 24-h modulation patterns," *Sci. Rep.*, vol. 12, no. 1, p. 15070, Sep. 2022.

[34] C. Meisel, R. El Atrache, M. Jackson, S. Schubach, C. Ufongene, and T. Loddenkemper, "Machine learning from wristband sensor data for wearable, noninvasive seizure forecasting," *Epilepsia*, vol. 61, no. 12, pp. 2653–2666, Dec. 2020.

[35] P. Boon et al., "A prospective, multicenter study of cardiac-based seizure detection to activate vagus nerve stimulation," *Seizure*, vol. 32, pp. 52–61, Nov. 2015.

[36] J. van Andel et al., "Multimodal, automated detection of nocturnal motor seizures at home: Is a reliable seizure detector feasible?" *Epilepsia Open*, vol. 2, no. 4, pp. 424–431, Dec. 2017.

[37] Y. Ge et al., "Multimodal wearable device signal based epilepsy detection with multi-scale convolutional neural network," in *Proc. Int. Conf. Cogn. Syst. Signal Process.* Cham, Switzerland: Springer, Nov. 2023, pp. 70–80.